A&A 529, A107 (2011)
DOI: 10.1051/0004-6361/201015365

Astronomy & Astrophysics

Photometry and models of selected main belt asteroids

VIII. Low-pole asteroids⋆,⋆⋆

A. Marciniak[1], T. Michałowski[1], M. Polińska[1], P. Bartczak[1], R. Hirsch[1], K. Sobkowiak[1], K. Kamiński[1], M. Fagas[1], R. Behrend[2], L. Bernasconi[3], J.-G. Bosch[4], L. Brunetto[5], F. Choisay[6], J. Coloma[7], M. Conjat[8], G. Farroni[6], F. Manzini[9], H. Pallares[7], R. Roy[10], T. Kwiatkowski[1], A. Kryszczyńska[1], R. Rudawska[1], S. Starczewski[11], J. Michałowski[12], and P. Ludick[13]

[1] Astronomical Observatory, Adam Mickiewicz University, Słoneczna 36, 60-286 Poznań, Poland
e-mail: aniab@lab.astro.amu.edu.pl
[2] Geneva Observatory, 1290 Sauverny, Switzerland
[3] Les Engarouines Observatory, 84570 Mallemort-du-Comtat, France
[4] Collonges Observatory, 90 allée des résidences, 74160 Collonges, France
[5] "Le Florian", Villa 4, 880 chemin de Ribac-Estagnol, 06600 Antibes, France
[6] AUDE Association (User association of electronic detectors) Paris, France
[7] Agrupación Astronómica de Sabadell, Apartado de Correos 50, PO Box 50, 08200 Sabadell, Barcelona, Spain
[8] l'Observatoire de Cabris, 408 chemin Saint Jean Pape, 06530 Cabris, France
[9] Stazione Astronomica di Sozzago, 28060 Sozzago, Italy
[10] Blauvac Observatory, 84570 St-Estève, France
[11] N. Copernicus Astronomical Centre, Polish Academy of Sciences, Bartycka 18, 00-716 Warsaw, Poland
[12] Forte Software, Os. Jagiełły 28/28 60-685 Poznań, Poland
[13] Ludick Observatory, Krugersdorp, South Africa

Received 8 July 2010 / Accepted 16 February 2011

ABSTRACT

Context. The set of more than 100 asteroids, for which spin parameters have been modelled using an amplitude, magnitude or epoch methods, showed a pronounced gap in the distribution of the asteroid spin axes. These spin axes are rarely aligned with the ecliptic plane.
Aims. The number of asteroids with known spin parameters should be increased to allow for statistical investigations.
Methods. We gathered extensive photometric datasets on four selected main-belt asteroids to model their spin and shape parameters using the *lightcurve inversion* method. Our only criterion of selection was their observability for small telescopes.
Results. All four of the modelled asteroids happened to have rotational poles that lie close to the ecliptic plane (periods and J2000 north pole coordinates): (94) Aurora – $P = 7.226191$ h, $\lambda_{p1} = 58°$, $\beta_{p1} = +16°$; $\lambda_{p2} = 242°$, $\beta_{p2} = +4°$; (174) Phaedra – $P = 5.750249$ h, $\lambda_p = 265°$, $\beta_p = +5°$; (679) Pax – $P = 8.456016$ h, $\lambda_{p1} = 42°$, $\beta_{p1} = -5°$; $\lambda_{p2} = 220°$, $\beta_{p2} = +32°$ (pole 2 preferred after comparison with AO-resolved observations); (714) Ulula – $P = 6.998376$ h, $\lambda_{p1} = 42°$, $\beta_{p1} = -9°$; $\lambda_{p2} = 227°$, $\beta_{p2} = -14°$.
Conclusions. This work suggests that asteroid spin axes do not avoid the ecliptic plane, contrary to what the classical modelling suggested.

Key words. techniques: photometric – minor planets, asteroids: general

1. Introduction

The traditional, long photometric observing runs of asteroids are no very time-efficient method, but remain the most abundant source of information we can infer from disk-integrated brightness measurements of these small bodies. Because thermal recoil forces (first described theoretically by Yarkovsky, and developed by Radzievskii 1954; Paddack 1969; and Rubincam 2000) were found to play a substantial role in asteroid dynamics and evolution (Kaasalainen et al. 2007; Lowry et al. 2007; Ďurech et al. 2008), there appeared more need for well determined asteroid pole and shape models. Therefore, to further increase the DAMIT,[1] and "Poznań" database[2], we present four new asteroid models obtained with the *lightcurve inversion* method.

This sample is different from the previous ones (included in Michałowski et al. 2004, 2005, 2006; Marciniak et al. 2007, 2008, 2009a,b) in the way that it contains only objects with poles of low inclination with respect to the ecliptic. These asteroids were long thought to be nonexistent, because modelling with the amplitude, magnitude, and epoch methods (Zappala & Di Martino 1986, and references therein) did not result in asteroid models with poles lying in the proximity of the

⋆ Composite lightcurves (Figs. 1–26), and aspect data (Table 1) are only available in electronic form at http://www.aanda.org
⋆⋆ Photometric data are only available in electronic form at the CDS via anonymous ftp to cdsarc.u-strasbg.fr (130.79.128.5) or via http://cdsarc.u-strasbg.fr/viz-bin/qcat?J/A+A/529/A107

[1] Database of Asteroid Models from Inversion Techniques, available at: http://astro.troja.mff.cuni.cz/projects/asteroids3D, described in Ďurech et al. (2010).
[2] A regularly updated database of all published asteroid spin parameters obtained with various techniques available at: http://www.astro.amu.edu.pl/Science/Asteroids (Kryszczyńska et al. 2007).

Table 2. Asteroid parameters.

Asteroid	D(km)	Albedo	Type	a(AU)	e	i(°)	Ω(°)
(94) Aurora	168.88	0.057	C	3.1611	0.088	7.96	2.70
(174) Phaedra	69.24	0.149	S	2.8591	0.145	12.13	327.74
(679) Pax	51.47	0.166	K	2.5866	0.311	24.38	112.30
(714) Ulula	39.18	0.271	S	2.5358	0.056	14.26	233.94

ecliptic plane (having low $|\beta_p|$ values). However, Marciniak & Michałowski (2010) showed that these objects apparently do exist, only these methods were not capable of reproducing their spin axes position well. Since the *lightcurve inversion* method (Kaasalainen & Torppa 2001; and Kaasalainen et al. 2001) does not make any assumption on the shape of an asteroid, complex shapes are possible, and they can exhibit brightness variations even when viewed pole-on.

2. Photometry of four main-belt asteroids

Since 1997 we have been conducting photometric observations at the Borowiec station of the Poznań Astronomical Observatory in Poland. The equipment is a 0.4-m Newtonian telescope with a ST-7 CCD camera (see Michałowski et al. 2004, for the description of our observing routine and the reduction procedures). This resulted in an extensive dataset of lightcurves coming from many apparitions. More efficient asteroid modelling became possible after we included data obtained at the Southern Hemisphere and those coming from amateur astronomers. An asteroid needs to be observed at a large span of viewing geometries, including well-spread ecliptic longitudes, and a big span of phase angles, to present a unique spin and shape model.

The asteroids (94) Aurora, (174) Phaedra, (679) Pax and (714) Ulula were observed during a total of 134 runs. Unfortunately, these are mainly short pieces of their lightcurves, owing to the weather or other limitations. That is why creating composite lightcurves (shown in Figs. 1–26) became necessary. This step saves time in applying the lightcurve inversion routine, because it narrows the spin period range that needs to be scanned. Changes in the lightcurve amplitude and shape owing to the changing phase angle can be noticed; they bear valuable information on the asteroid's shape and its shadowing properties, so we applied no corrections to this effect.

Table 1 contains the aspect data for all the observing runs. The mid-time of observation and the distances to the Earth and Sun in Astronomical Units are indicated in the first two columns. The table also shows the corresponding Sun-object-Earth phase angle and the J2000 ecliptic latitude and longitude of an asteroid in the sky. The next two columns provide data on the length and quality of each lightcurve, in the form of the number of points and the standard deviation in the relative brightnesses of one comparison star relative to another, usually the brightest ones in the image. The last column provides the observatory code.

Table 2 contains the physical parameters of these asteroids, including their diameters, albedos, taxonomic types and orbital parameters[3,4].

[3] Data for these properties come from *The Small Bodies Node of the NASA Planetary Data System* http://pdssbn.astro.umd.edu/), where the diameters and albedos are from the IRAS Minor Planet Survey (Tedesco et al. 2004), and the taxonomic classifications are given after Bus & Binzel (2002).

[4] The data on orbital parameters come from the Minor Planet Center database available at: ftp://cfa-ftp.harvard.edu/pub/MPCORB/MPCORB.DAT

2.1. (94) Aurora

Asteroid (94) Aurora's lightcurve was first presented by Harris & Young (1983). The data came from three nights in late August 1979 and were composited with 7.22 h period, showing regular 0.12 mag light variations. In 1984 Di Martino et al. (1987) observed over one night one full revolution of (94) Aurora, assuming the period of 7.22 h. This time the amplitude was also 0.12 mag, but the lightcurve was less regular, with one minimum visibly lower than the other. These were the only observations of this object from the southern Earth hemisphere. Schevchenko et al. (2006) and Marchis et al. (2006) refined the albedo and diameter values to 169 km and 0.0446; and to 168.88 km respectively.

Our observations of (94) Aurora spanned six apparitions: 1998, 1999, 2004, 2005, 2008, and 2009/2010. In many cases almost flat lightcurves were observed, so it was difficult to confirm its rotation period, not to mention any modelling attempts (see Figs. 1 to 6). The last apparition changed the situation, because (94) Aurora then displayed relatively large amplitudes (0.18 mag), and good quality lightcurves were obtained over a long period of time (see the composite lightcurve in Fig. 6). All composits were created using the period of 7.226 h, thus confirming previous determinations.

2.2. (174) Phaedra

Magnusson & Lagerkvist (1991) observed (174) Phaedra on two consecutive nights in March 1987 at ESO, obtaining 5.75 ± 0.05 h period and a 0.53 mag amplitude. Sada & Cooney (2001) and Wang & Shi (2002) observed this asteroid in the year 2001. The first group obtained 5 runs, spanning one month at the beginning of 2001, and successfully composited them with a period of 5.744 ± 0.001 h. The lightcurve was highly asymmetric, with one minimum 0.2 mag deeper than the other. The other group observed (174) Phaedra later, on two nights close in time in March 2001. They obtained a similar period, 5.74 ± 0.01 h and slightly larger, overall amplitude of 0.40 mag. In 2003 Ivarsen et al. (2004) obtained data for (174) Phaedra with large amplitude of 0.52 mag, suggesting again a 5.75 ± 0.01 h period. On five nights in November 2008 more observations of this object were made by Ruthroff (2009), resulting in confirmation of the 5.75 h period.

We included lightcurve data in our modelling from the first three mentioned works since the other ones were unavailable.

We gathered lightcurves of (174) Phaedra on eight apparitions: 1998, 2000, 2001, 2005, 2006, 2007, 2008, and 2010 (see Table 1). This asteroid exhibited profound changes in its lightcurves: from simple, bimodal ones through the lightcurves of deep and shallow minima to monomodal, low-amplitude ones (Figs. 7 to 14). The amplitudes ranged from 0.18 to 0.58 mag, and the period of 5.750 h was the only one that could fit the entire set of composite lightcurves.

2.3. (679) Pax

The first lightcurve of (679) Pax was presented in Schober (1981). Two-night data came from October 1978 and were made at ESO in Chile using a photometer. The small-amplitude (0.07 mag) lightcurve was composited with a period 7.625 ± 0.005 h, but another period of 8.472 h could not be completely ruled out yet. No variations in colour during rotation were noticed. Another set of data on (679) Pax also comes from ESO and was published by Schober et al. (1994). In September 1982, it was observed during three nearby nights. This time

Table 3. Spin models parameters with their error values. See Sect. 3 for a description of the columns of this table.

Sidereal	Pole 1		Pole 2		Pole_{orb} 1		Pole_{orb} 2		Observing span	N_{app}	N_{lc}	Method	Reference
period (h)	λ_p	β_p	λ_p	β_p	λ_o	β_o	λ_o	β_o	(years)				
(94) Aurora													
7.226191	58°	+16	242°	+4°	56°	+9	239°	+11°	1979–2010	8	21	L	Present work
±0.000005	±5°	±8°	±5°	±8°	±5°	±8°	±5°	±8°					
(174) Phaedra													
5.750249		–	265°	+5°		–	298°	+16°	1987–2010	9	36	L	Present work
±0.000003		–	±1°	±1°		–	±1°	±1°					
(679) Pax													
	65°	−5	245°	+5°					1978–2005	5	12	AM	Shevchenko et al. (2009)
8.456016	42°	−5	220°	+32°	291°	+18	105°	+8°	1978–2010	8	42	L	Present work
±0.000006	±5°	±5°	±5°	±5°	±5°	±5°	±5°	±5°					
(714) Ulula													
6.99838	40°	−4°	225°	−13°					1983–2004	1*	4	L(com)	Ďurech et al. (2009)
6.998377	42	−9	227°	−14°	171	−12	350°	−12°	1983–2009	7	40	L	Present work
±0.000002	±2°	±2°	±1°	±1°	±2°	±2°	±1°	±1°					

Notes. (*) 1 appartition with a few dense lightcurves + around hundred sparse data points.

the lightcurve was symmetric, with a much larger amplitude of 0.32 mag, and the period determination yielded a value of 8.452 ± 0.003. Next, Chiorny et al. (2003) confirmed this period. Marchis et al. (2006), using the W. M. Keck adaptive optics, estimated the general dimensions of this asteroid to be 78×47 km. Shevchenko et al. (2009) obtained a 0.15 mag light variation on three nights in May 1998, and composited these data with a 8.452 h period. Using data previously published, they estimated a pole position (see Table 3) with the nominal error of ±2° and with the ellipsoid axes values of $a/b = 1.18$ and $b/c = 1.30$.

We used photometric data extracted from the first two works and our recently acquired data for the modelling of the shape by lightcurve inversion.

We gathered data from six apparitions: 2002, 2004, 2005, 2006, 2009, and 2010. (679) Pax could only be observed in four limited places in its orbit, displaying only two states: large (around 0.30 mag); or very small (around 0.05 mag) amplitude lightcurves, without the intermediate stages. The composite lightcurves shown in Figs. 15 to 20 were created using the period of 8.4570 h, similar to the ones found by other authors.

2.4. (714) Ulula

Schober and Stadler (1990) observed (714) Ulula photoelectrically during four nights in January 1983 at ESO, obtaining a 0.55 mag lightcurve with sharp minima. The data were composited with a 7.000 ± 0.005 h period. Photometric measurements for this target from the year 2005 were published by Lichelli (2006). Again, an amplitude of 0.55 mag was measured, and the synodic period was found to be 6.998 ± 0.001 h. Ďurech et al. (2009) published a model of this asteroid using the modified lightcurve inversion method, based mostly on sparse absolute brightness measurements. Their result is shown in Table 3.

We also extensively observed (714) Ulula in 2005 apparition, so we merged our data with the lightcurves from the first paper only.

Our database contains six apparitions for (174) Ulula: 2001, 2004, 2005, 2006, 2008, and 2009. Here also a commensurability with the Earth motion was present, so the apparitions of this asteroid took place in three places in its orbit only. In one of them practically flat lightcurves were observed, while in two others amplitudes of some 0.60 and 0.40 mag were noticed (see Figs. 21 to 26). The period found to fit all the composits, 6.9982 h, agrees with previous estimates.

3. Pole and shape results

All the studied objects exhibit clear signs of a low pole orientation ("low" in a sense of the ecliptic latitude, the $|\beta_p|$ value). In some apparitions lightcurves of substantial amplitude were observed, while in other small or almost no brightness variations were exhibited by the same object. This implies that these asteroids must have been sometimes viewed nearly pole-on. These asteroids are more problematic for modelling, because the rotation period cannot be determined well on flat lightcurves. But if other apparitions are well covered, this problem can be overcome.

We perform our asteroid modelling with the *lightcurve inversion* method described in Kaasalainen & Torppa (2001) and Kaasalainen et al. (2001). It allows the determination of both the pole and period solutions and the recovery of an approximated convex shape model. To mimic the surface reflectivity of the asteroids, we used a standard combination of Lommel-Seeliger and Lambert scattering laws, and to construct a convex reperesentatin of the shape model we used a spherical harmonics expansion, as described in the above-mentioned papers.

In Table 3 we present the parameters of the four models compared to previous results, if there are any. The first column contains the sidereal period with its uncertainty. The next four columns present the pole solutions (J2000 ecliptic longitude λ_p and latitude β_p), with a "mirror" pole solution, because the uncertainty on two symmetrical pole solutions cannot be removed for asteroids that orbit close to the ecliptic plane. The pole solutions were also recalculated with respect to each asteroid's orbital plane and placed in the next four columns (λ_o and β_o). Usually, an asteroid ecliptic pole latitude is similar to its orbital pole latitude, because the orbit inclinations are not high for main-belt asteroids. However, with this sample of low-lying poles, the difference becomes important, thus we give both the ecliptic and orbital poles for future investigations.

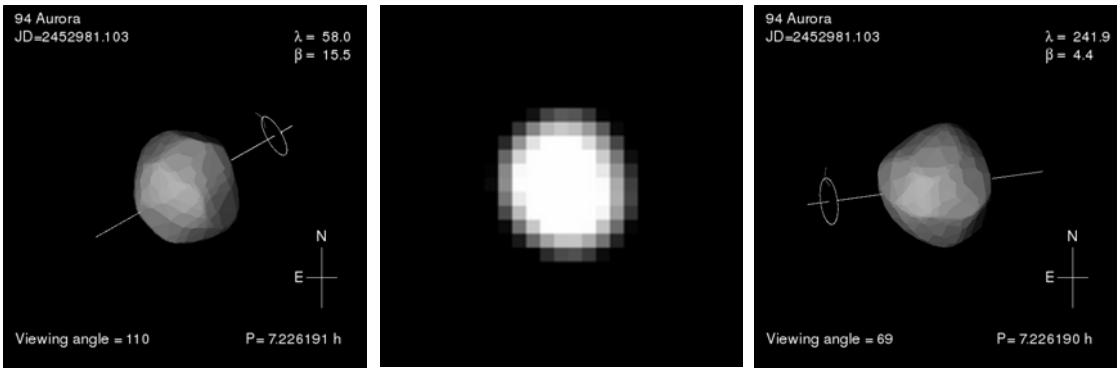

Fig. 27. Shape models of the Pole 1 and Pole 2 solutions for (94) Aurora (*left* and *right* image, respectively) compared to the Marchis' et al. (2006) adaptive optics image (*middle*) at the same epoch and viewing geometry.

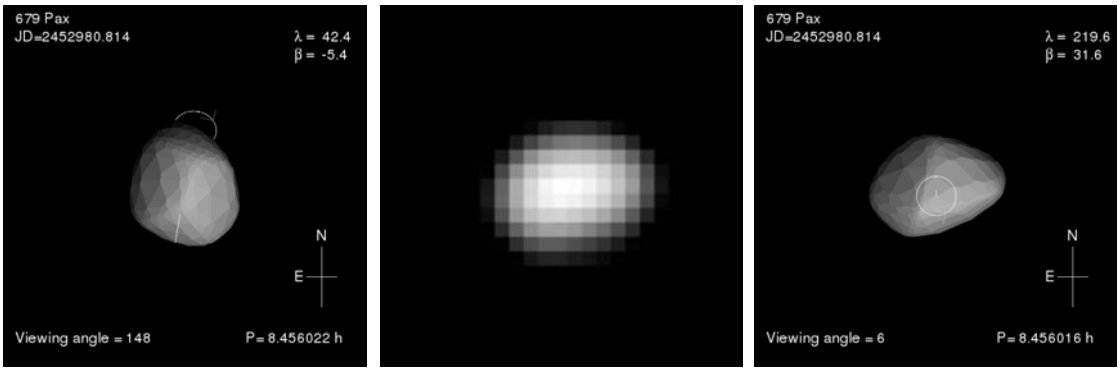

Fig. 28. Shape models of the Pole 1 and Pole 2 solutions for (679) Pax (*left* and *right* image, respectively) compared to the Marchis' et al. (2006) adaptive optics image (*middle*) at the same epoch and viewing geometry.

For each of the ecliptic pole coordinates, a separate error analysis was performed, because errors in this method can only be estimated from the resulting parameter space (see Torppa et al. 2003; and Kaasalainen & Ďurech 2007, for more details). The error values are indicated in the second row of each asteroid solution. The next three columns of Table 3 contain the observing span in years, the number of all apparitions ($N_{\rm app}$) and the number of lightcurves ($N_{\rm lc}$) used for the modelling. In the two last columns, the method used ("L" for lightcurve inversion) is indicated and its reference.

To present how the model lightcurves reproduce the observed ones, we display in Figs. 29, 31, 33, and 35 three example observing runs, each from a different apparition (black dots), compared to the fits produced by the model (solid lines). The aspect angles of the Earth and the Sun (ϕ and ϕ_0), and phase angle α are also given. The corresponding shape models are displayed in Figs. 30, 32, 34, and 36.

3.1. (94) Aurora

The model of (94) Aurora was constructed from 21 lightcurves from 8 apparitions (1979, 1984, 1998, 1999, 2004, 2005, 2008, and 2009/2010). The latest apparition, with a large span of the observing dates (from December until May!) and the phase angles (7° to 18°) proved to be crucial for obtaining a unique model. (94) Aurora then displayed large amplitudes in a lightcurve of a small scatter. All these factors influenced the quality of the solution shown in Table 3.

To obtain good fits to the observations, the degree and order of the spherical harmonics expansion needed to be increased, and many stray points had to be removed, because noisy lightcurves can spoil the solution or make it unretrievable. A compact shape model and the lightcurve fits are shown in Figs. 30 and 29, respectively.

In Fig. 27 we compare both our models with the adaptive optics image from Marchis et al. (2006). Unfortunately, because of the rather regular look of (94) Aurora in this viewing geometry, none of the solutions can be excluded on this basis.

3.2. (174) Phaedra

(174) Phaedra was a difficult case. Although we were able to find one unique sidereal period and a preliminary pole solution on a relatively small dataset, the model fit to the observed lightcurves and shape model appearance were unsatisfactory. The biggest problem was the shape model's dimensions, where the z-axis was not coincident with the principal axis of the inertia tensor. The only solution to that problem was to add more photometric data. We created a 3D-shape convex model based on 36 lightcurves from 9 apparitions (1987, 1998, 2000, 2001, 2005, 2006, 2007, 2008, and 2010). Such a large dataset permitted the rejection of the mirror pole solution, since the fit of some of the lightcurves was poor and the shape models did not look "physical". As another consequence we obtained an unusually small error of the final pole position on the celestial sphere (see Table 3).

Some lightcurves had to be averaged, to influence the solution with similar weight as the data coming from other apparitions. As a result, all model lighcurves fit the observations well (Fig. 31) and the shape model (Fig. 32) is irregular, as expected from the changes in the pattern of the lightcurve.

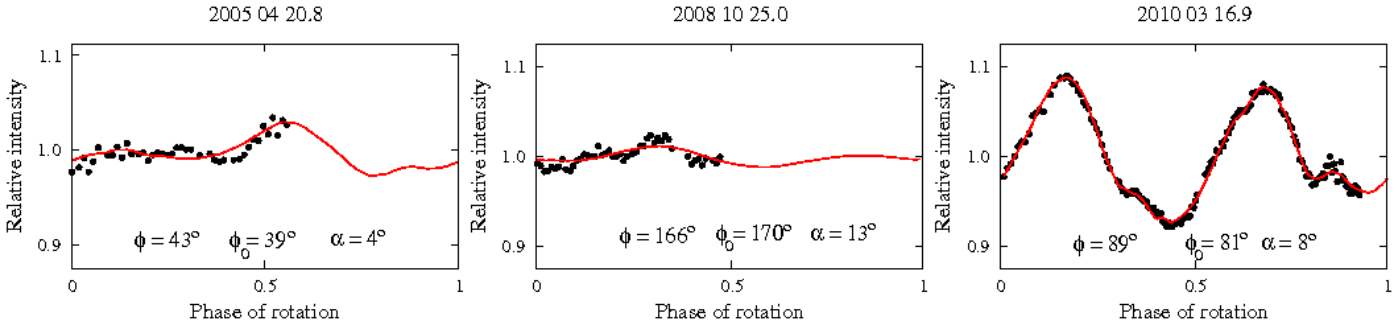

Fig. 29. Observed lightcurves (points) superimposed on the lightcurves created by a model (curves) at the same epochs for (94) Aurora. The overall rms residual of the fit was 0.0105 mag.

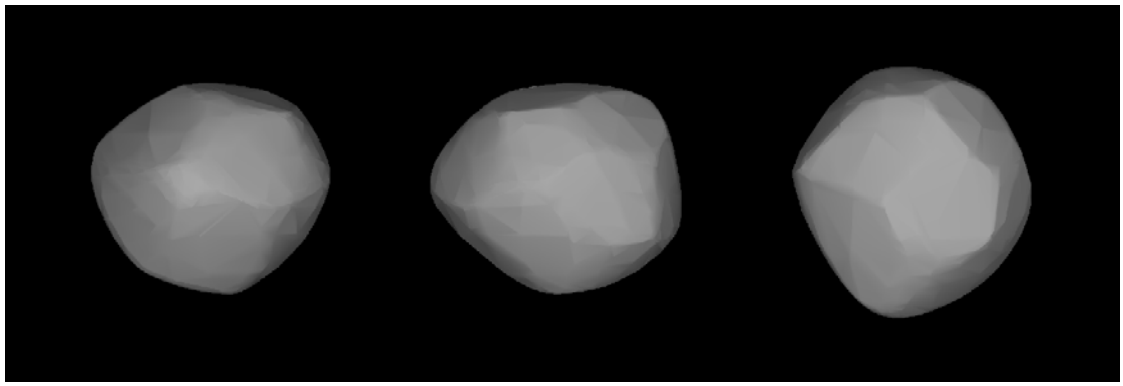

Fig. 30. Approximated convex shape model of (94) Aurora, shown at equatorial viewing and illumination geometry, with rotational phases 90° apart (two pictures on the left), and the pole-on view on the right. The reflectivity law is artificial, to reveal the shape details.

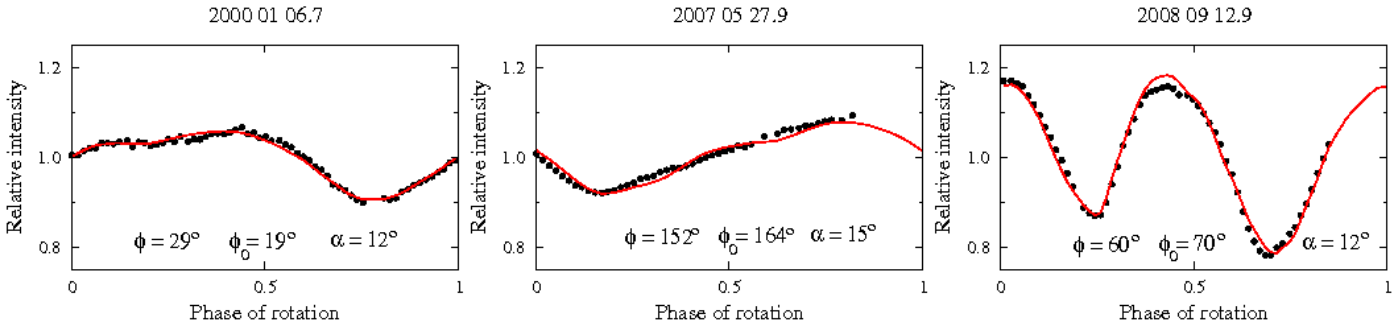

Fig. 31. Observed versus modelled lightcurves for (174) Phaedra. The rms residual was 0.0172 mag.

3.3. (679) Pax

The orbital motion of (679) Pax is commensurable with the Earth's in terms of a mean motion, so the observing geometries were very limited. Still, it was possible to construct its model based on 42 lightcurves from 8 apparitions: 1978, 1982, 2002, 2004, 2005, 2006, 2009, and 2010. The pole coordinates are presented in Table 3.

Two more periods and some other pole orientations could provide a good numerical solution, but the visual assessment clearly proved these solutions wrong, as they gave time shifts or artificial lightcurve features compared to the observing points, especially in the last apparition in 2010 (unlike the adopted one shown in Fig. 33). The resulting elongated shape model is presented in Fig. 34.

The model obtained here confirms one of the solutions previously found by Shevchenko et al. (2009), while disagreeing with the other. However, our solutions are based on a richer dataset, and are consequently probably more reliable (see Table 3).

We also compared this model to the image of (679) Pax from AO observations made by Marchis et al. (2006), Fig. 28. Owing to the small aspect angle, the orientation of the model mostly depends on the phase of rotation, which is tied to the sidereal period. Assuming the period obtained here is correct, the comparison to the AO image suggests that the second solution (λ_p = 220°, β_p = +32°) is preferred.

3.4. (714) Ulula

We constructed the model of asteroid (714) Ulula from a set of 40 partially averaged lightcurves from 7 apparitions: 1983, 2001, 2004, 2005, 2006, 2008, and 2009. A strongly preferred solution for the spin period and spin axis orientation was found in the solution space (see Table 3), but owing to the restricted viewing

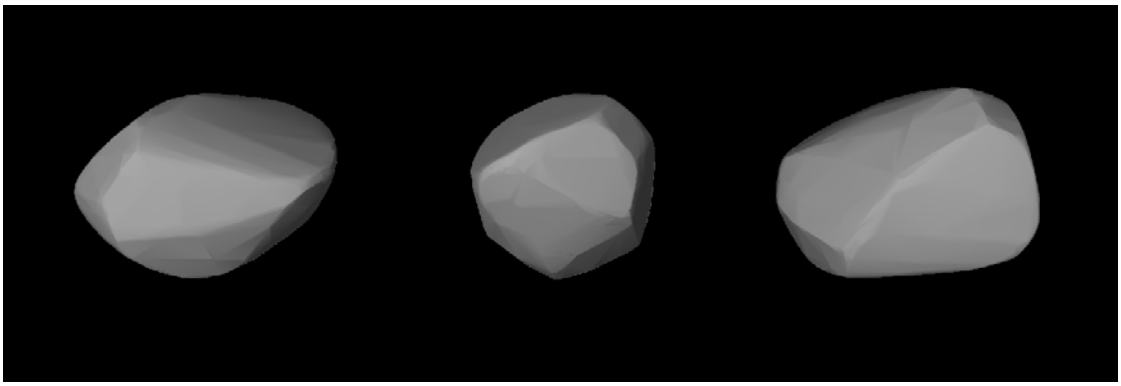

Fig. 32. Shape model of (174) Phaedra.

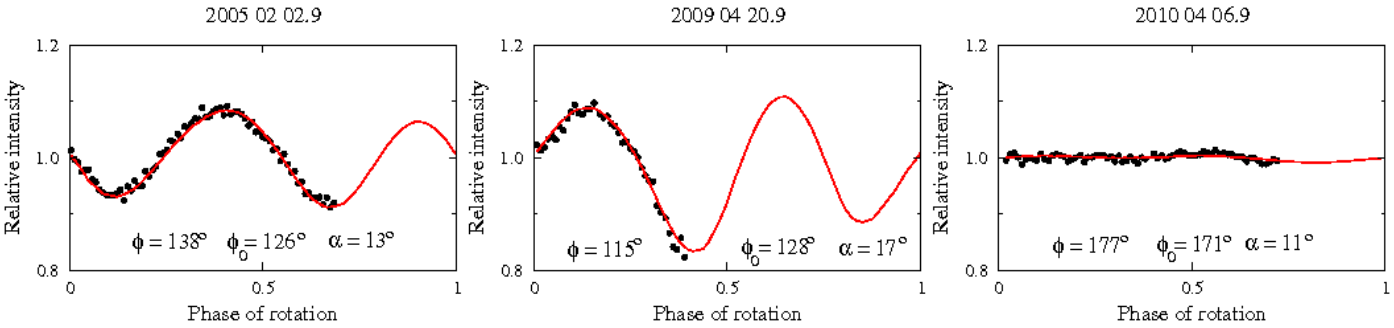

Fig. 33. Observed versus modelled lightcurves for (679) Pax. The rms residual was 0.0117 mag.

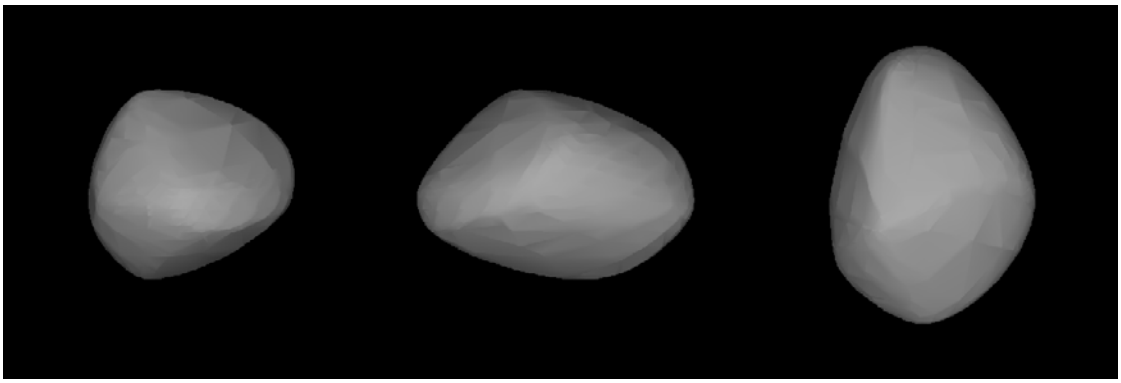

Fig. 34. Shape model of (679) Pax.

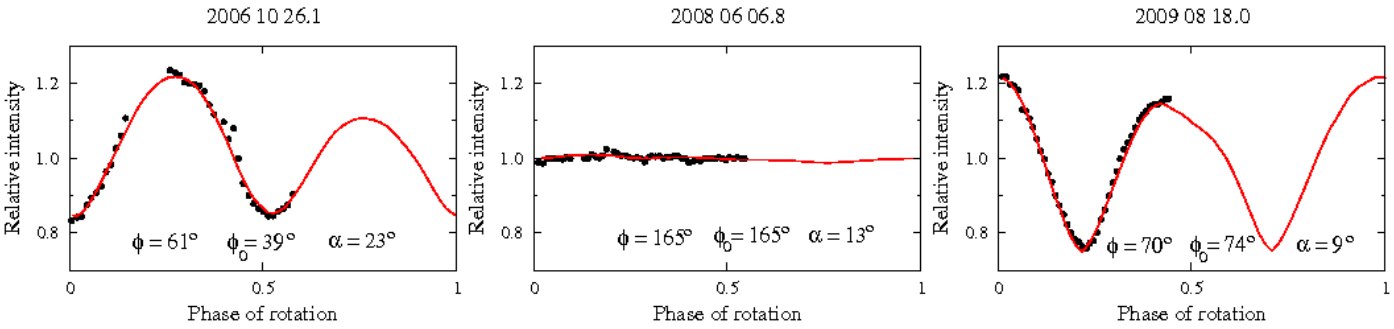

Fig. 35. Observed versus modelled lightcurves for (714) Ulula. The rms residual was 0.0210 mag.

geometry, the shape model may have a slightly wrong inertia tensor in the *c*-axis direction (up to ±5%, see Fig. 36). The model fit to the observed lightcurves is shown in Fig. 35.

This model closely agrees with that of Ďurech et al. (2009), thus firming the reliability of a modified lightcurve inversion method, which combines a small number of dense lighcturves with many sparse data points.

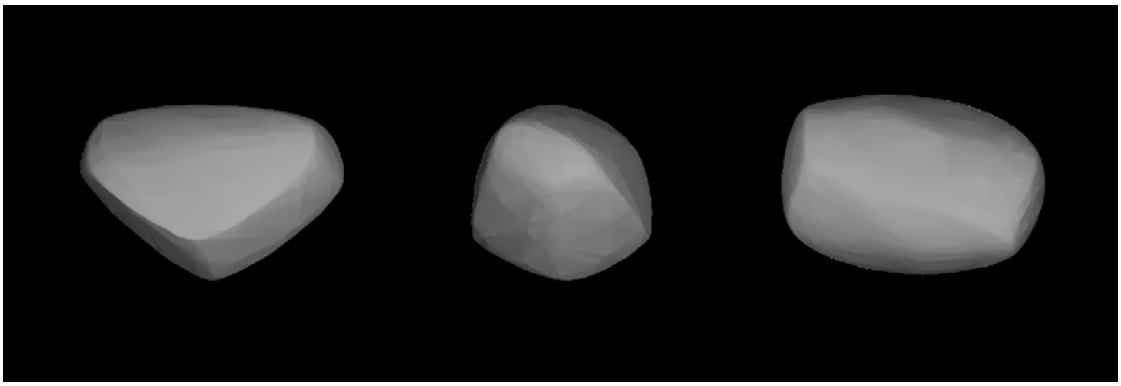

Fig. 36. Shape model of (714) Ulula.

4. Discussion and conclusion

Modelling of these asteroids with the classical EAM methods would most probably give higher $|\beta_p|$ values, because a smooth ellipsoid cannot exhibit brightness variations when viewed pole-on. It is possible that the observed ecliptic gap, with β_p values from +8 to −8, mentioned by Pravec et al. (2002) and Kryszczyńska et al. (2007) is in fact due to the use of inaccurate EAM methods. Indeed, if the asteroid spin axes were randomly oriented, the histograms included in these works should be flat. The lack of asteroids with a low inclination with respect to the ecliptic remained an unexplained observational fact.

Marciniak & Michałowski (2010) have shown that this gap could be artificial, caused by the aforementioned EAM methods' bias and by averaging various authors' results in the spin axis database. These four convex 3D shape models of main-belt asteroids presented here further confirm that lowly-inclined asteroids exist in the solar system. This work complements the database of asteroids with known spin parameters that we are currently building. Today this set contains slightly more than one hundred asteroids. It is still not enough to draw conclusions on the spin axis of various sub-groups of asteroids by statistical analysis.

Acknowledgements. Borowiec observations were reduced with the *CCLRS STARLINK* package. This work was partially supported by grants No. N N203 302535 and N N203 404139 from the Polish Ministry of Science and Higher Education. This work is partially based on observations made at the South African Astronomical Observatory (SAAO). The *lightcurve inversion* code was designed by Mikko Kaasalainen and modified by Josef Ďurech. It is available at http://astro.troja.mff.cuni.cz/projects/asteroids3D.

References

Bus, S. J., & Binzel, R. P. 2002, Icarus, 158, 146
Chiorny, V. G., Shevchenko, V. G., Krugly, Yu. N., et al. 2003, Abstracts of Photometry and Polarimetry of Asteroids: Impact on Collaboration, Kharkiv, 9
Di Martino, M., Zappala, V., de Campos, J. A., Debehogne, H., & Lagerkvist, C.-I. 1987, A&AS, 67, 95
Ďurech, J., Vokrouhlicky, D., Kaasalainen, M., et al. 2008, A&A, 489, L25
Ďurech, J., Kaasalainen, M., Warner, B., et al. 2009, A&A, 493, 291
Ďurech, J., Sidorin, V., & Kaasalainen, M. 2010, A&A, 513, A46
Harris, A. W., & Young, J. W. 1983, Icarus, 54, 59
Ivarsen, K., Willis, S., Ingleby, L., et al. 2004, Minor Planet Bull., 31, 29
Kaasalainen, M., & Ďurech, J. 2007, in Near Earth Objects, our Celestial Neighbors: Opportunity and Risk, ed. A. Milani, G. B. Valsecchi, & D. Vokrouhlicky (Cambridge: Cambridge University Press), 151
Kaasalainen, M., & Torppa, J. 2001, Icarus, 153, 24
Kaasalainen, M., Torrpa, J., & Muinonen, K. 2001, Icarus, 153, 37
Kaasalainen, M., Ďurech, J., Warner, B. D., et al. 2007, Nature, 446, 420
Kryszczyńska, A., La Spina, A., Paolicchi, P., et al. 2007, Icarus, 192, 223
Licchelli, D. 2006, Minor Planet Bull., 33, 11
Lowry, S. C., Fitzsimmons, A., Pravec, P., et al. 2007, Science, 316, 272
Magnusson, P., & Lagerkvist, C.-I. 1991, A&AS, 87, 269
Marchis, F., Kaasalainen, M., Hom, E. F. Y., et al. 2006, Icarus, 185, 39
Marciniak, A., & Michałowski, T. 2010, A&A, 512, A56
Marciniak, A., Michałowski, T., Kaasalainen, M., et al. 2007, A&A, 473, 633
Marciniak, A., Michałowski, T., Kaasalainen, M., et al. 2008, A&A, 478, 559
Marciniak, A., Michałowski, T., Hirsch, R., et al. 2009a, A&A, 498, 313
Marciniak, A., Michałowski, T., Hirsch, R., et al. 2009b, A&A, 508, 1503
Michałowski, T., Kwiatkowski, T., Kaasalainen, M., et al. 2004, A&A, 416, 353
Michałowski, T., Kaasalainen, M., Marciniak, A., et al. 2005, A&A, 443, 329
Michałowski, T., Kaasalainen, M., Polińska, M., et al. 2006, A&A, 459, 663
Paddack, S. J. 1969, J. Geophys. Res., 74, 4379
Pravec, P., Harris, A. W., & Michałowski, T. 2002, in Asteroids III, ed. W. Bottke, A. Cellino, P. Paolicchi, & R. P. Binzel (Tucson: Univ. of Arizona Press), 113
Radzievskii, V. V. 1954, Dokl. Akad. Nauk SSSR, 97, 49
Rubincam, D. P. 2000, Icarus, 148, 2
Ruthroff, J. C. 2009, Minor Planet Bull., 36, 121
Sada, P. V., & Cooney, W. 2001, Minor Planet Bull., 28, 39
Shevchenko, V. G., & Tedesco, E. F. 2006, Icarus, 184, 211
Shevchenko, V. G., Tungalag, N., Chiorny, V. G., et al. 2009, Planet. Space Sci., 57, 1514
Schober, H. J. 1981, A&A, 99, 199
Schober, H. J., & Stadler, M. 1990, A&A, 230, 233
Schober, H. J., Erikson, A., Hahn, G., et al. 1994, A&AS, 105, 281
Tedesco, E. F., Noah, P. V., Noah, M., & Price S. D. 2004, IRAS Minor Planet Survey. IRAS-A-FPA-3-RDR-IMPS-V6.0, NASA Planetary Data System
Tholen, D. J. 1989, in Asteroids II, ed. R. P. Binzel, T. Gehrels, & M. S. Matthews (Univ. Arizona Press), 1139
Torppa, J., Kaasalainen, M., Michalowski, T., et al. 2003, Icarus, 164, 346
Wang, X.-B., & Shi, Y. 2002, Earth, Moon and Planets, 91, 181
Zappala, V., & Di Martino, M. 1986, Icarus, 68, 40

Pages 8 to 14 are available in the electronic edition of the journal at http://www.aanda.org

Table 1. Aspect data.

Date (UT)	r (AU)	Δ (AU)	Phase angle (°)	λ (J2000) (°)	β (°)	N_p	σ (mag)	Obs.
(94) Aurora								
1998-02-07.9	2.9514	2.2923	16.21	82.80	10.24	42	0.040	Bor
1998-02-17.8	2.9566	2.4156	17.80	83.14	9.69	18	0.020	Bor
1998-02-21.9	2.9588	2.4687	18.29	83.45	9.46	28	0.005	Bor
1999-03-01.0	3.2342	2.2665	4.50	174.59	2.52	53	0.006	Bor
2004-04-02.9	3.0737	2.6703	18.37	117.86	6.70	34	0.008	Bor
2004-04-13.8	3.0823	2.8274	18.91	119.33	6.13	15	0.004	Bor
2004-04-21.8	3.0886	2.9440	18.99	120.73	5.74	27	0.006	Bor
2004-04-29.9	3.0950	3.0604	18.82	122.36	5.38	21	0.009	Bor
2005-04-18.9	3.3549	2.3686	3.84	196.43	−3.37	21	0.090	Bor
2005-04-20.9	3.3560	2.3760	4.50	196.06	−3.42	42	0.008	Bor
2008-10-24.1	2.8828	2.0520	12.91	70.51	9.20	50	0.004	Bor
2008-10-25.1	2.8828	2.0436	12.62	70.41	9.26	47	0.010	Bor
2009-12-03.1	3.0745	2.8694	18.68	158.56	5.85	57	0.020	Bor
2010-03-16.9	3.1629	2.2392	7.96	150.51	4.69	162	0.011	Bor
2010-04-06.8	3.1807	2.4301	13.67	148.30	3.74	57	0.004	Bor
2010-05-13.7	3.2116	2.9251	18.19	150.02	2.22	32	0.007	SAAO
2010-05-15.8	3.2133	2.9549	18.25	150.30	2.15	62	0.006	SAAO
(174) Phaedra								
1998-10-18.8	2.8907	2.0480	12.53	347.07	9.06	50	0.018	Bor
1998-10-19.8	2.8922	2.0584	12.81	346.97	9.06	30	0.010	Bor
2000-01-06.8	3.2707	2.4938	12.11	63.68	15.25	66	0.006	Bor
2000-01-08.8	3.2708	2.5139	12.56	63.48	15.10	21	0.004	Bor
2000-01-12.8	3.2710	2.5551	13.39	63.16	14.80	37	0.008	Bor
2000-01-13.8	3.2711	2.5657	13.58	63.09	14.72	41	0.005	Bor
2001-02-14.8	2.9919	2.0094	2.36	139.27	2.02	11	0.010	Bor
2001-03-01.8	2.9716	2.0450	8.16	136.10	1.12	10	0.015	Bor
2005-01-16.9	3.2684	2.4865	12.02	74.93	14.08	28	0.003	Bor
2005-02-01.9	3.2643	2.6585	15.16	73.96	12.81	31	0.008	Bor
2005-02-06.8	3.2629	2.7191	15.87	73.96	12.41	60	0.007	Bor
2006-01-28.0	2.9326	2.0475	10.12	159.40	−0.43	36	0.008	Bor
2006-04-19.8	2.8123	2.2101	18.55	146.73	−4.68	9	0.020	Bor
2006-04-20.9	2.8108	2.2208	18.73	146.76	−4.71	20	0.020	Bor
2006-04-24.9	2.8048	2.2642	19.37	146.93	−4.82	41	0.008	Bor
2006-04-27.8	2.8048	2.2642	19.37	146.93	−4.82	18	0.020	Bor
2006-05-04.9	2.7898	2.3769	20.58	147.77	−5.06	19	0.038	Bor
2007-05-24.0	2.4457	1.6003	16.20	282.07	−16.45	27	0.011	SAAO
2007-05-28.0	2.4467	1.5717	14.98	281.74	−16.59	46	0.007	SAAO
2008-09-13.0	3.0114	2.1617	12.13	27.70	12.70	57	0.006	Bor
2008-09-25.8	3.0279	2.0957	8.41	25.64	13.65	19	0.014	Bor
2008-09-26.1	3.0284	2.0944	8.31	25.58	13.67	15	0.014	Bor
2008-09-27.8	3.0305	2.0888	7.82	25.24	13.78	41	0.004	Bor
2008-09-28.8	3.0317	2.0861	7.55	25.06	13.84	8	0.005	Bor
2008-10-04.8	3.0394	2.0739	5.96	23.79	14.17	35	0.020	Bor
2010-01-22.9	3.2432	2.4099	10.74	86.75	12.76	36	0.004	Bor
2010-01-31.9	3.2387	2.4890	12.92	85.75	12.08	21	0.006	Bor
2010-04-16.8	3.1889	3.4443	16.84	93.56	6.88	27	0.008	Bor
2010-04-18.8	3.1873	3.4688	16.67	94.06	6.78	22	0.016	Bor
2010-04-25.8	3.1815	3.5526	15.99	95.89	6.43	18	0.010	Bor
(679) Pax								
2002-03-30.1	3.1949	2.6102	16.12	248.19	26.83	19	0.019	Bor
2002-04-04.1	3.1859	2.5462	15.52	248.03	27.29	21	0.012	Bor
2002-04-06.0	3.1824	2.5225	15.26	247.93	27.45	5	0.010	Bor
2002-04-08.0	3.1786	2.4978	14.98	247.80	27.63	14	0.007	Bor
2002-05-07.0	3.1219	2.2295	10.25	243.18	29.21	9	0.011	Bor
2002-05-08.0	3.1198	2.2235	10.11	242.94	29.22	24	0.018	Bor
2002-05-09.0	3.1178	2.2177	9.98	242.70	29.23	36	0.028	Bor
2002-05-10.0	3.1158	2.2124	9.86	242.46	29.23	28	0.021	Bor
2002-05-11.0	3.1136	2.2069	9.74	242.21	29.23	45	0.007	Bor
2002-05-18.0	3.0988	2.1770	9.19	240.42	29.11	45	0.008	Bor
2002-05-18.9	3.0968	2.1740	9.16	240.18	29.08	13	0.011	Bor
2004-01-03.8	1.9350	1.2839	27.03	42.66	−26.18	29	0.013	Soz
2005-02-01.0	3.1287	2.3718	13.31	173.35	24.92	33	0.020	Bor
2005-02-01.1	3.1289	2.3712	13.28	173.34	24.93	59	0.007	Soz

Table 1. continued.

Date (UT)	r	Δ	Phase angle	λ (J2000)	β	N_p	σ	Obs.
	(AU)	(AU)	(°)	(°)	(°)		(mag)	
2005-02-03.0	3.1329	2.3586	12.89	173.04	25.22	75	0.007	Soz
2005-02-05.1	3.1371	2.3462	12.46	172.70	25.53	42	0.003	Bor
2005-02-09.1	3.1450	2.3251	11.65	171.98	26.08	37	0.013	EnO
2005-02-28.2	3.1814	2.2790	8.71	167.51	28.09	13	0.008	Bor
2005-03-20.0	3.2163	2.3358	9.73	162.34	28.72	40	0.006	Bor
2005-03-31.0	3.2342	2.4107	11.62	159.96	28.44	56	0.003	Bor
2005-04-03.1	3.2391	2.4365	12.18	159.40	28.30	22	0.050	Bor
2005-04-04.1	3.2406	2.4453	12.36	159.24	28.25	24	0.007	Bor
2006-03-23.1	3.2958	2.6793	15.14	237.16	28.93	35	0.004	Bor
2006-03-24.1	3.2946	2.6672	15.02	237.10	29.04	27	0.005	Bor
2006-04-06.1	3.2776	2.5269	13.20	235.89	30.29	33	0.011	Bor
2006-04-07.1	3.2762	2.5172	13.05	235.75	30.38	36	0.004	Bor
2006-04-27.1	3.2474	2.3686	10.15	231.88	31.51	24	0.011	Bor
2009-04-11.0	3.1441	2.5027	15.77	146.21	24.27	43	0.018	Bor
2009-04-16.1	3.1539	2.5684	16.46	146.04	23.95	27	0.010	Bor
2009-04-21.0	3.1634	2.6360	17.03	146.02	23.61	40	0.009	Bor
2009-04-25.0	3.1710	2.6924	17.41	146.12	23.33	30	0.012	Bor
2009-05-19.9	3.2151	3.0592	18.34	148.58	21.64	32	0.006	Bor
2009-05-27.9	3.2282	3.1787	18.18	149.95	21.15	33	0.009	Bor
2010-03-03.2	3.3689	2.8671	15.81	226.92	28.78	18	0.007	Bor
2010-03-26.9	3.3521	2.6082	12.91	225.35	31.48	6	0.014	Bor
2010-04-07.0	3.3427	2.5211	11.30	223.46	32.42	71	0.006	Bor
2010-06-16.9	3.2595	2.6409	15.78	209.34	28.33	28	0.014	Bor
(714) Ulula								
2001-09-21.8	2.6041	1.6923	11.47	335.38	20.92	7	0.060	Coll
2001-09-26.9	2.6014	1.7176	12.84	334.48	20.42	15	0.030	Coll
2001-10-10.8	2.5939	1.8150	16.54	332.84	18.75	28	0.048	AUDE
2001-10-11.9	2.5933	1.8235	16.79	332.77	18.62	21	0.050	Coll
2001-10-12.0	2.5932	1.8246	16.82	332.76	18.61	18	0.050	Cabr
2001-10-12.9	2.5927	1.8327	17.05	332.71	18.48	71	0.051	AUDE
2001-10-13.0	2.5927	1.8330	17.06	332.71	18.48	54	0.041	LFA
2001-10-13.9	2.5922	1.8407	17.27	332.67	18.36	61	0.055	AUDE
2004-05-16.0	2.6160	1.6092	2.63	228.71	−1.17	48	0.016	EnO
2005-10-23.8	2.5927	1.9891	20.04	328.57	17.06	71	0.019	AUDE
2005-10-24.8	2.5922	1.9993	20.19	328.62	16.94	37	0.020	Sab
2005-10-27.7	2.5905	2.0309	20.62	328.83	16.56	36	0.010	Bor
2005-10-27.8	2.5905	2.0317	20.63	328.84	16.55	30	0.018	AUDE
2005-10-28.8	2.5900	2.0420	20.75	328.92	16.43	30	0.020	Bor
2005-10-29.8	2.5893	2.0536	20.89	329.01	16.30	39	0.008	Bor
2005-10-30.8	2.5888	2.0643	21.01	329.11	16.18	30	0.004	Bor
2005-10-31.8	2.5883	2.0756	21.12	329.21	16.05	30	0.004	Bor
2005-11-04.9	2.5859	2.1229	21.56	329.70	15.54	29	0.030	AUDE
2005-11-07.9	2.5842	2.1586	21.83	330.14	15.16	20	0.020	Sab
2005-11-11.8	2.5819	2.2056	22.11	330.78	14.69	53	0.017	Bla
2006-10-26.1	2.4004	1.8943	23.16	103.99	−8.22	37	0.009	Bor
2006-10-27.0	2.3941	1.5675	16.00	104.94	−12.78	30	0.028	Bor
2006-12-02.1	2.3933	1.5302	14.31	104.36	−13.53	60	0.011	Bor
2008-06-06.8	2.6200	1.7342	13.34	219.86	−0.38	52	0.006	SAAO
2009-08-10.0	2.6365	1.6993	10.48	335.17	22.41	46	0.018	Lud
2009-08-17.0	2.6335	1.6780	9.14	333.60	22.62	36	0.004	SAAO
2009-08-18.0	2.6331	1.6759	8.99	333.35	22.64	45	0.005	SAAO
2009-09-07.9	2.6238	1.6893	10.25	328.36	22.09	17	0.008	Bor
2009-09-08.9	2.6234	1.6925	10.47	328.15	22.03	31	0.012	Bor
2009-09-14.8	2.6206	1.7172	11.96	326.96	21.56	24	0.005	Bor
2009-09-16.8	2.6196	1.7273	12.48	326.60	21.38	19	0.005	Bor
2009-09-17.8	2.6192	1.7326	12.75	326.43	21.29	24	0.007	Bor
2009-09-18.8	2.6187	1.7380	13.01	326.27	21.19	8	0.003	Bor
2009-09-19.8	2.6182	1.7441	13.29	326.11	21.09	12	0.004	Bor
2009-09-26.9	2.6148	1.7906	15.14	325.18	20.34	23	0.006	Bor
2009-09-27.8	2.6144	1.7973	15.38	325.08	20.24	8	0.005	Bor

Notes. Observatory Code: Bor – Borowiec; SAAO – South African Astronomical Observatory; Soz – Stazione Astronomica di Sozzago; EnO – Les Engarouines Observatory; Coll – Collonges Observatory; AUDE – AUDE Association; Cabr – Cabris, France; LFA – "Le Florian", Antibes; Sab – Sabadell, Barcelona; Bla – Blauvac Observatory; Lud – Ludick Observatory, Krugersdorp.

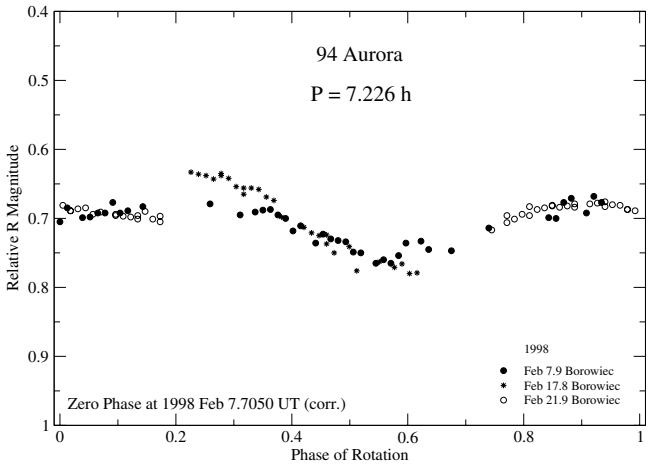

Fig. 1. Composite lightcurve of (94) Aurora in 1998.

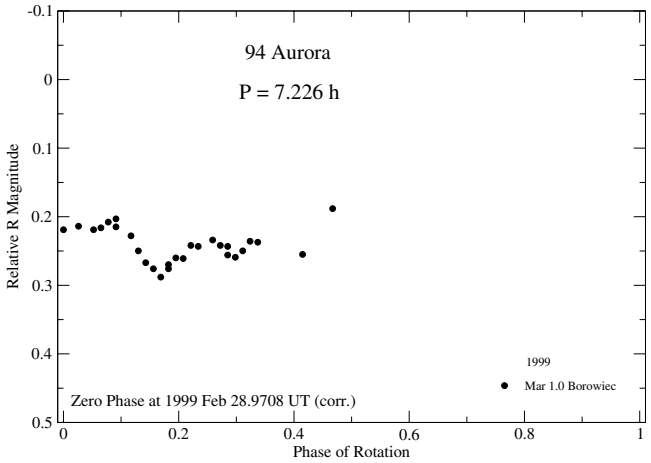

Fig. 2. Composite lightcurve of (94) Aurora in 1999.

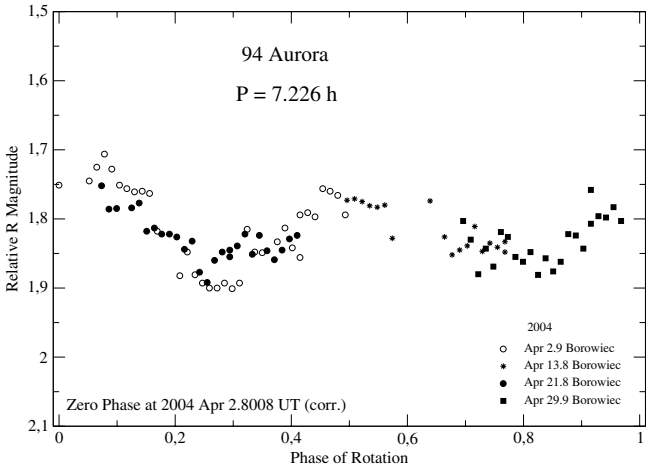

Fig. 3. Composite lightcurve of (94) Aurora in 2004.

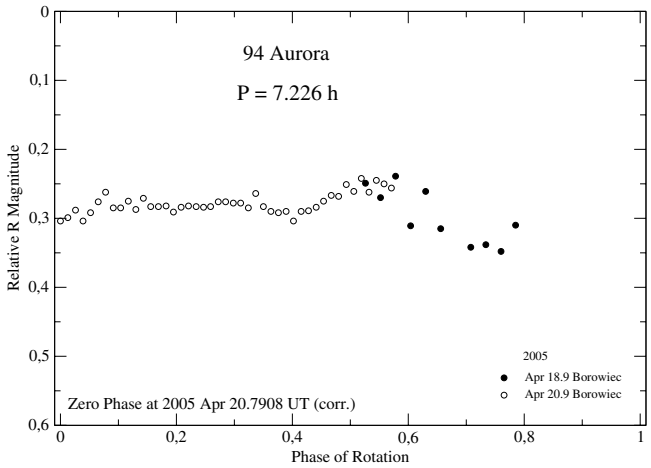

Fig. 4. Composite lightcurve of (94) Aurora in 2005.

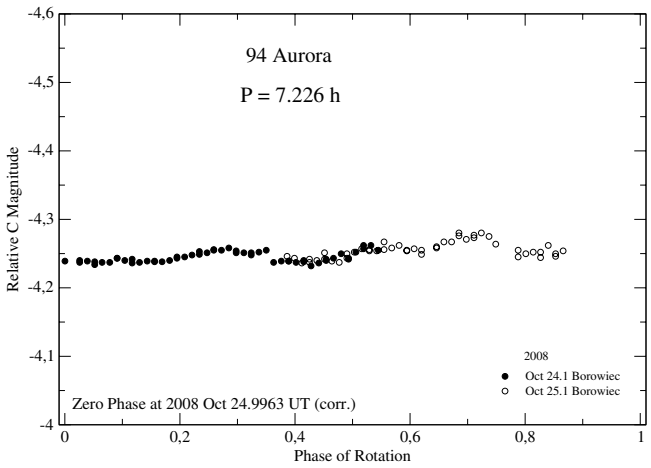

Fig. 5. Composite lightcurve of (94) Aurora in 2008.

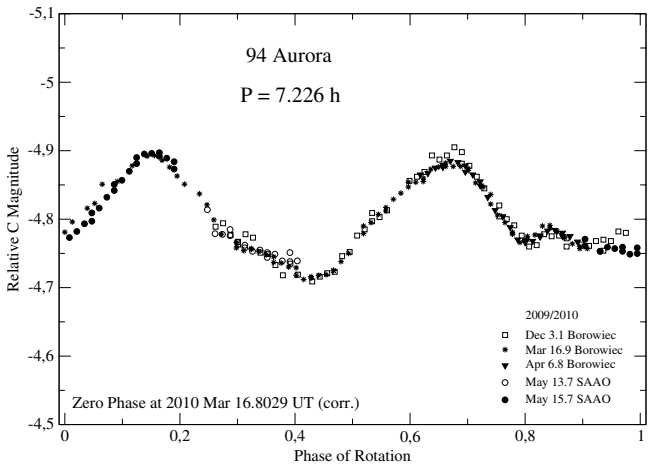

Fig. 6. Composite lightcurve of (94) Aurora in 2009−2010.

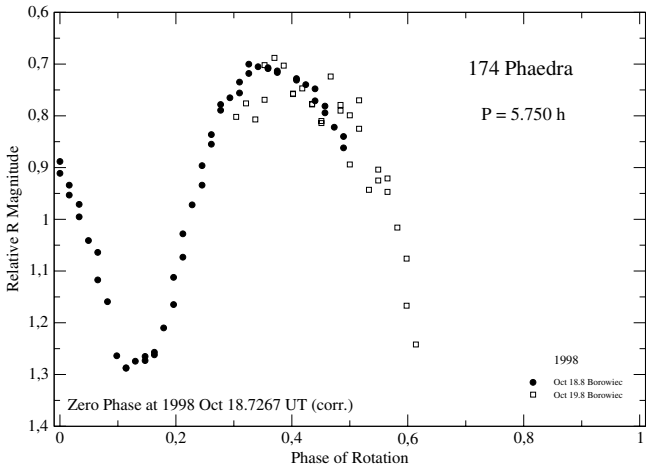

Fig. 7. Composite lightcurve of (174) Phaedra in 1998.

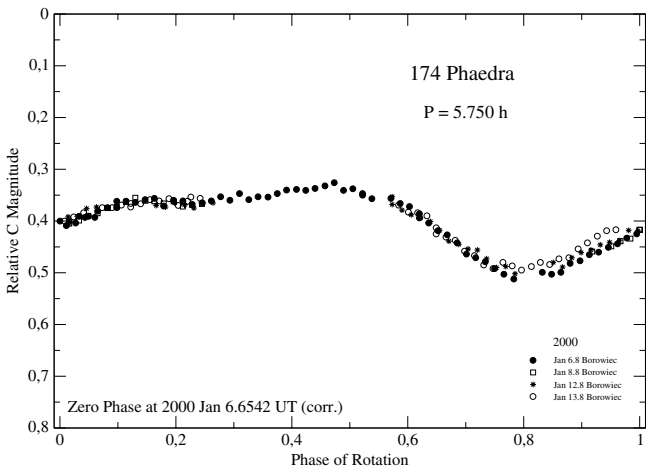

Fig. 8. Composite lightcurve of (174) Phaedra in 2000.

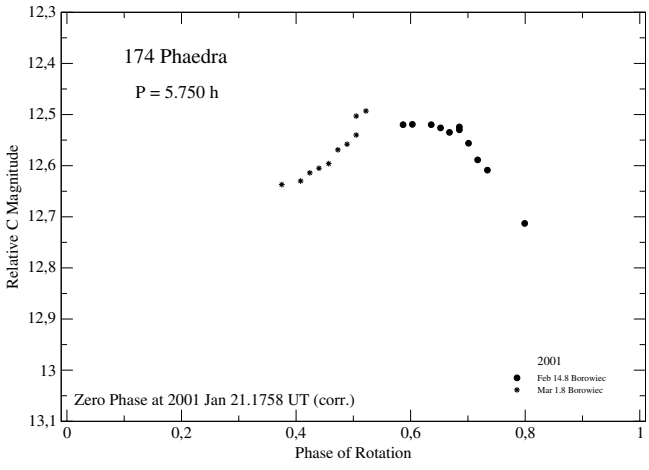

Fig. 9. Composite lightcurve of (174) Phaedra in 2001.

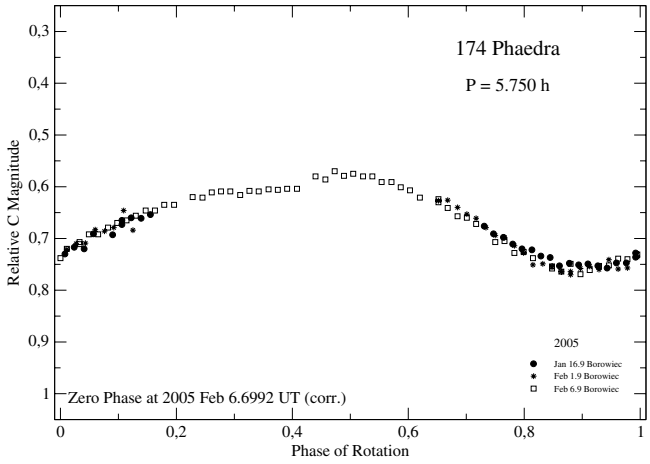

Fig. 10. Composite lightcurve of (174) Phaedra in 2005.

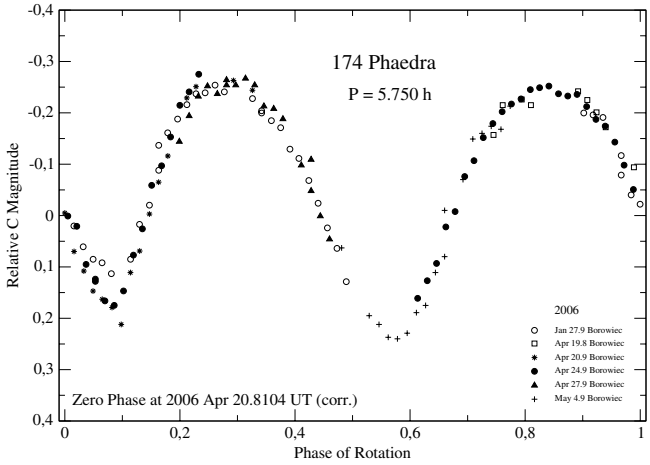

Fig. 11. Composite lightcurve of (174) Phaedra in 2006.

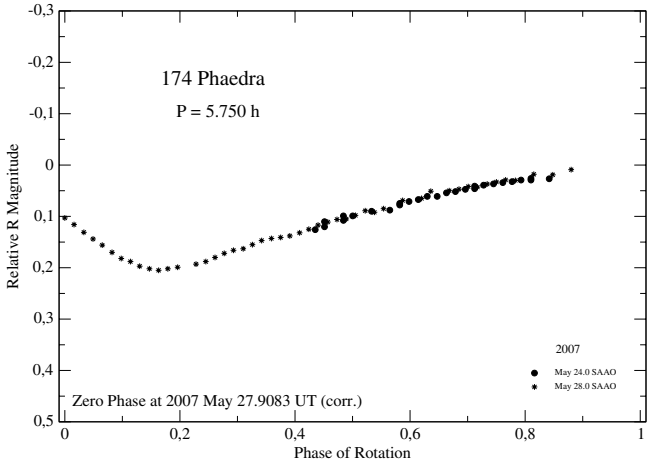

Fig. 12. Composite lightcurve of (174) Phaedra in 2007.

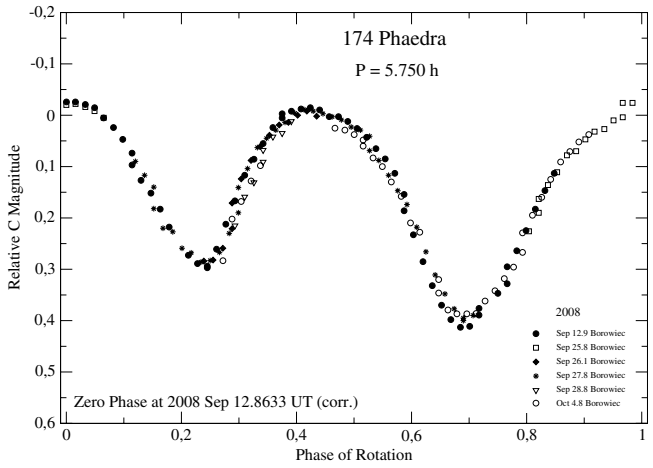

Fig. 13. Composite lightcurve of (174) Phaedra in 2008.

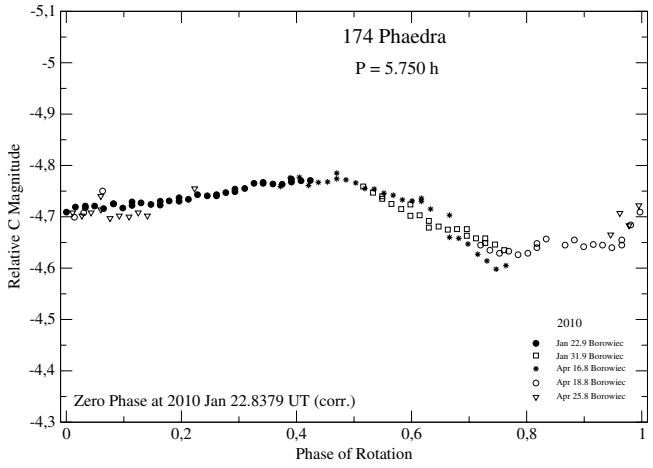

Fig. 14. Composite lightcurve of (174) Phaedra in 2010.

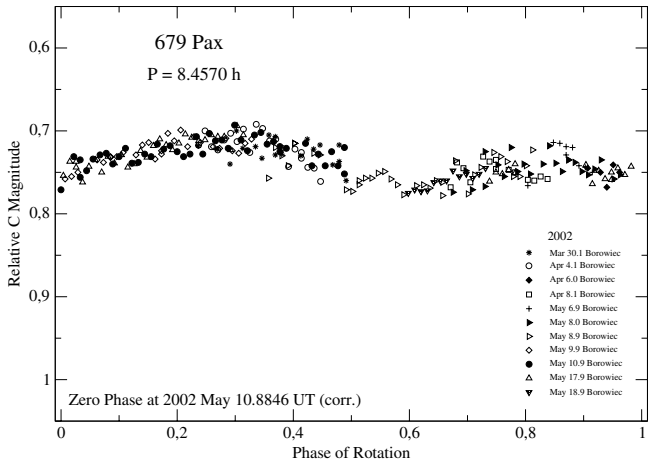

Fig. 15. Composite lightcurve of (679) Pax in 2002.

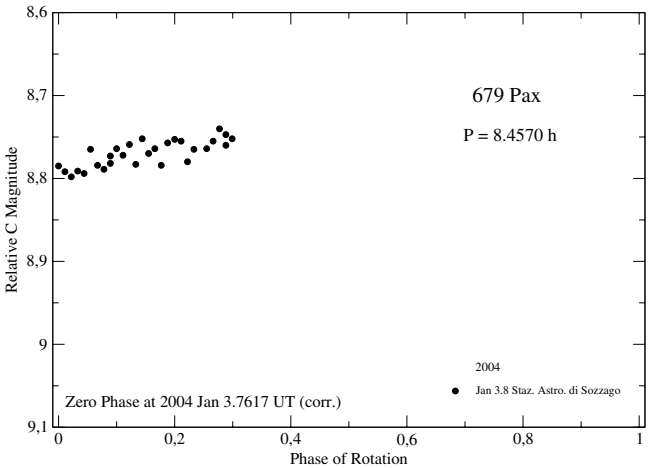

Fig. 16. Lightcurve of (679) Pax in 2004.

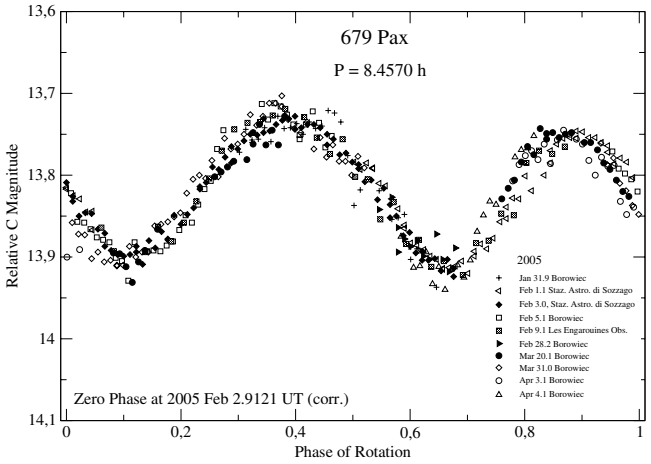

Fig. 17. Composite lightcurve of (679) Pax in 2005.

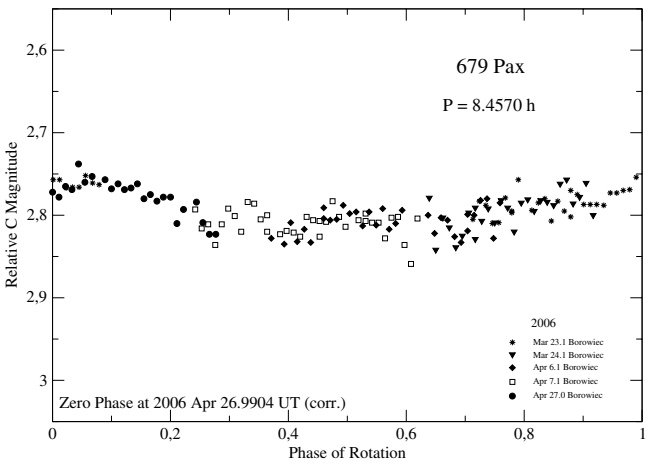

Fig. 18. Composite lightcurve of (679) Pax in 2006.

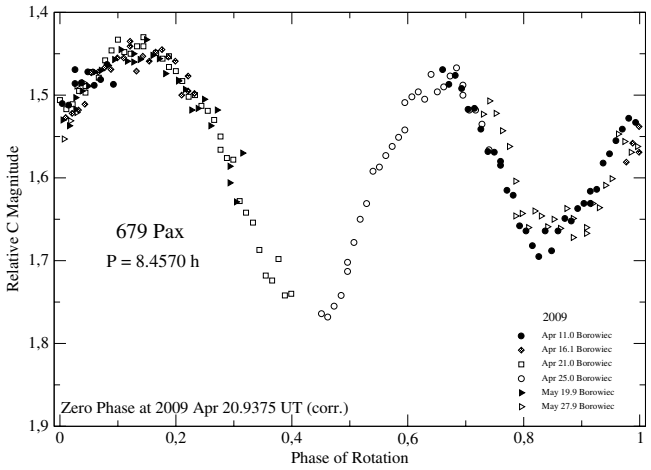

Fig. 19. Composite lightcurve of (679) Pax in 2009.

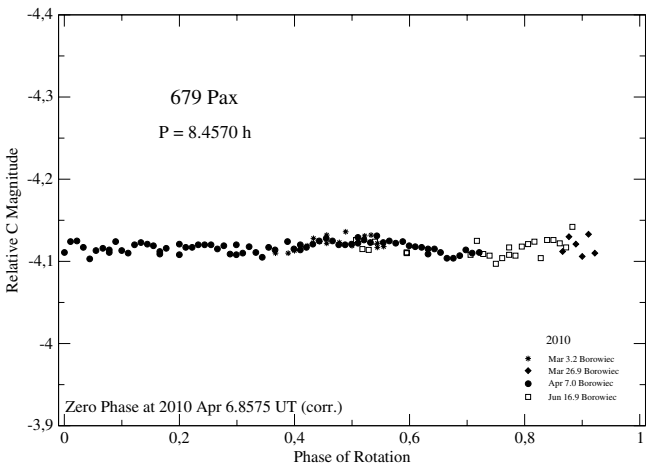

Fig. 20. Composite lightcurve of (679) Pax in 2010.

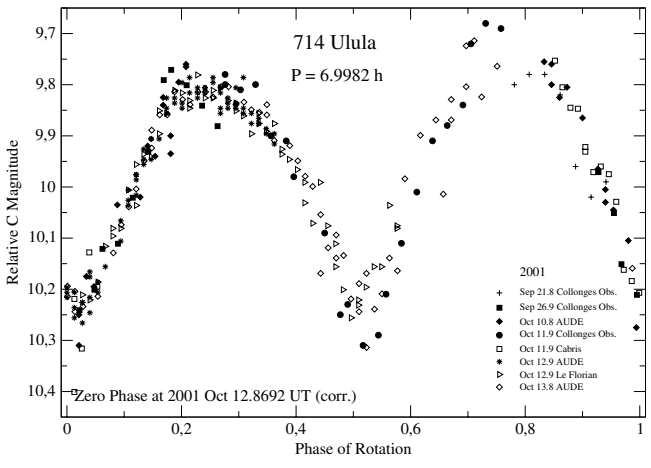

Fig. 21. Composite lightcurve of (714) Ulula in 2001.

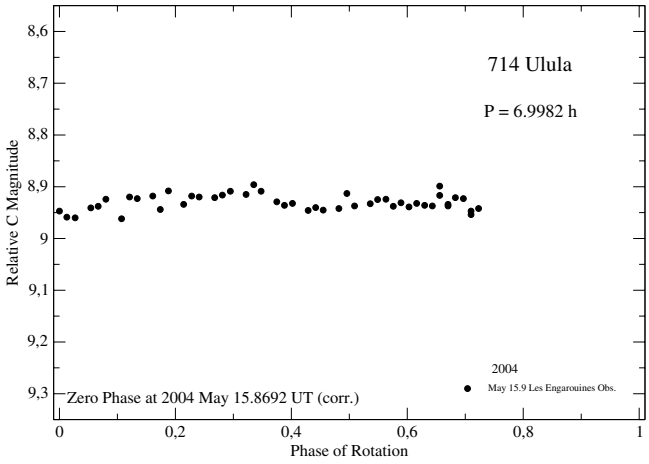

Fig. 22. Lightcurve of (714) Ulula in 2004.

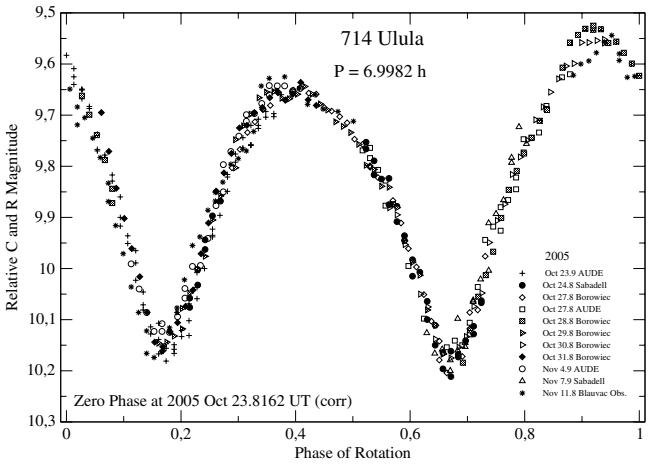

Fig. 23. Composite lightcurve of (714) Ulula in 2005.

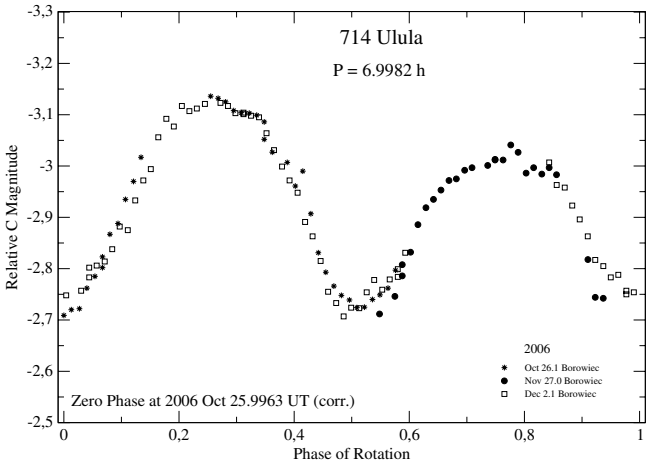

Fig. 24. Composite lightcurve of (714) Ulula in 2006.

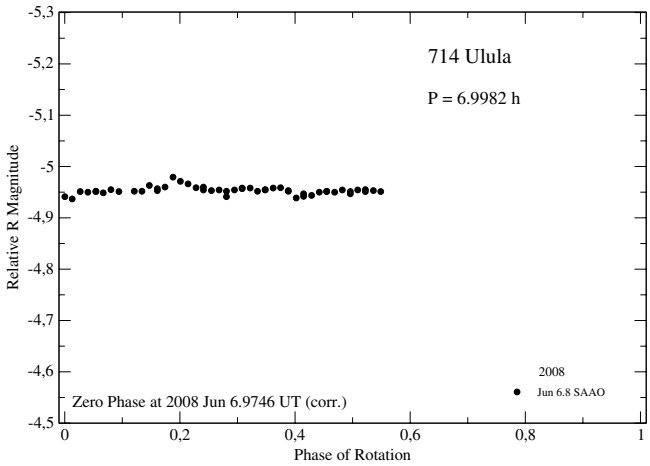

Fig. 25. Lightcurve of (714) Ulula in 2008.

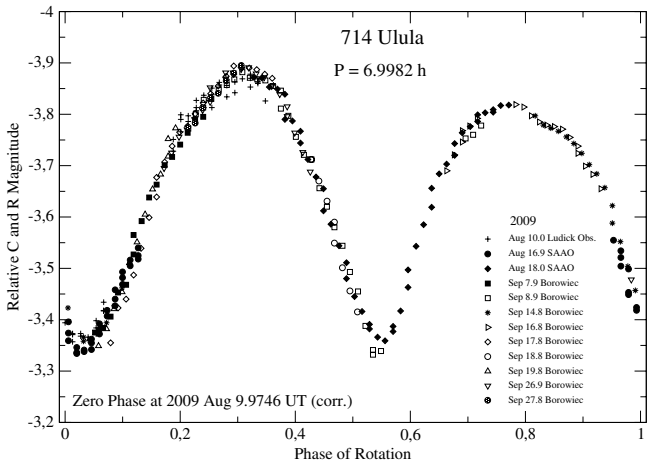

Fig. 26. Composite lightcurve of (714) Ulula in 2009.